Ecosystem development following deglaciation: A new sedimentary record from Devils Lake, Wisconsin, USA

Williams, Joseph J.; Mclauchlan, Kendra K.; Mueller, Joshua R.; Mellicant, Emily M.; Myrbo, Amy E.; Lascu, Ioan

Published in:
Quaternary Science Reviews

DOI:
10.1016/j.quascirev.2015.08.009

Publication date:
2015

Citation for published version (APA):
Williams, J. J., Mclauchlan, K. K., Mueller, J. R., Mellicant, E. M., Myrbo, A. E., & Lascu, I. (2015). Ecosystem development following deglaciation: A new sedimentary record from Devils Lake, Wisconsin, USA. *Quaternary Science Reviews*, *125*, 131-143. https://doi.org/10.1016/j.quascirev.2015.08.009

Ecosystem development following deglaciation: a new sedimentary record from Devils Lake, Wisconsin, USA

Joseph J. Williams[1*#], Kendra K. McLauchlan[1], Joshua R. Mueller[1], Emily M. Mellicant[2], Amy E. Myrbo[3] and Ioan Lascu[3,4,§]

[1] Department of Geography, Kansas State University, 118 Seaton Hall, Manhattan, Kansas, USA 66506

[2] Rosenstiel School of Marine and Atmospheric Science, University of Miami, 4600 Rickenbacker Causeway, Miami, Florida, USA 33149

[3] LacCore/CSDCO/Limnological Research Center, Department of Earth Sciences, University of Minnesota, 500 Pillsbury Drive SE, Minneapolis, Minnesota, USA 55455

[4] Institute for Rock Magnetism, Department of Earth Sciences, University of Minnesota, 100 Union Street SE, Minneapolis, Minnesota, USA 55455

* Present address: Department of Geography and Earth Sciences, Aberystwyth University, Aberystwyth, SY23 3DB, Wales, UK
[§] Present address: University of Cambridge, Department of Earth Sciences, Cambridge, CB2 3EQ, United Kingdom
[#] Corresponding author

Abstract

Processes and rates of ecosystem development can be reconstructed using lacustrine sedimentary sequences, but this approach requires records that contain the start of primary succession. Most lakes in the upper Midwestern U.S. were formed by glaciers at the end of the last Ice Age approximately 11,700 cal yr BP. Devils Lake, Wisconsin is a rare example of a lake from this region whose sediments extend into the Pleistocene and may include the Last Glacial Maximum (26,000 cal yr BP). Sediment magnetic, geochemical, pollen, and charcoal records were generated from a 10 meter core whose basal sediments may be 28,000 years old. Together with an earlier pollen record, these proxies combine to reveal a history of long-term climatic, vegetative and geologic change during the late Pleistocene to Holocene. We identify six sedimentary units that indicate a series of consecutive events rather than a predictable trajectory of ecosystem development at the site. Productivity in the lake was low during the late Pleistocene and increased during the Holocene, as reflected by the sediment lithology, which shows a sudden shift from glacial vivianite-rich and organic-poor clastic-dominated sediments to Holocene diatomaceous sapropels. Several important processes initiated around 17,000 cal yr BP, including the onset of organic matter accumulation and fire in the terrestrial ecosystem. However, the post-glacial landscape was not devoid of vegetation because pollen assemblages indicate that terrestrial vegetation, likely a spruce tundra, survived near the site. A switch to a hardwood forest period during the Holocene also led to a change in the fire regime, with increased frequency of burning. Aquatic ecosystem productivity lagged terrestrial ecosystem productivity throughout the record. Nutrient cycling (as recorded by sedimentary $\delta^{15}N$) was variable but not directional, and appeared to be correlated with climate conditions early in the record, and terrestrial ecosystem processes later in the record. Throughout the Holocene magnetic mineral concentration decreased as productivity increased, and the source of magnetic material shifted from almost exclusively lithogenic to approximately 50% derived from soil or biogenic sources. Magnetic grain size, *Ambrosia* pollen percentages, and charcoal concentration increased and $\delta^{15}N$ decreased in the most recent part of the record, due to anthropogenic influence in the region including agricultural activities.

Keywords: climate; vegetation; fire; Holocene; mineral magnetism; primary succession; stable isotopes

1. Introduction

Theories about the nature and mechanisms of ecosystem change have been developed from chronosequences (Jenny 1941), whereby sites substitute for time since the start of primary succession. Different absolute rates but similar sequences of biogeochemical events have been observed on chronosequences formed by a variety of processes such as aeolian transport, wildfire, volcanic lava flow, uplift of marine terraces, and glacial retreat (Wardle et al. 2004). Sedimentary archives have the potential to provide continuous records of ecosystem development with excellent chronological control. One of the few examples of a chronosequence paired with sedimentary palaeorecords focused on nutrient cycling in lakes and landscapes of Glacier Bay, Alaska following recent glacial retreat (Engstrom et al. 2000). In this case, although in a relatively cold climate, the entire sequence from bare rock to old-growth conifer forest took only ~150 years (Milner et al. 2007).

From individual sedimentary palaeorecords spanning several millennia, the main trajectories of ecosystem change seem to be establishment of vegetation and broadly predictable increases in ecosystem productivity, biomass, and nutrient availability. Thus, primary succession processes are dominated by accumulation of organic matter during the Holocene (Mourier et al. 2010), and sometimes much longer timescales (Finkenbinder et al. 2014), but the rates and controls of these processes are largely unknown. Trajectories of both eutrophication and dystrophication have been observed on Holocene timescales in sediments of oligotrophic lakes (Oldfield et al. 2010). Additionally, ecosystem feedbacks with fire regimes and the relative roles of vegetation and climate change on biogeochemical processes are not well studied. The most recent glaciation of North America, the retreat of the Laurentide Ice Sheet, and the formation of lakes with sedimentary sequences provide an opportunity to examine primary ecosystem development.

Devils Lake, Wisconsin, USA has been a key location for understanding long-term environmental changes across a transition zone between grassland and forest (Maher 1982). The lake and surrounding landscape underwent significant and complex changes during the last glacial period, followed by deglaciation and transition into the Holocene period (Attig et al. 2011). Earlier debate focused on the vegetation composition during the cool Younger Dryas (YD) interval (12.8 to 11.5 ka) (Baker et al. 1992, Shuman et al. 2002, Grimm et al. 2009). High temporal resolution pollen analysis provided a detailed vegetation history, which was primarily interpreted as responding to climate changes, but no other ecosystem proxies have been measured at this site. Importantly, Devils Lake is situated on the boundary between the glaciated and non-glaciated areas of southwestern Wisconsin. This non-glaciated terrain, known as the Driftless Area, contains very few sites with continuous deposition (Maher 1982), so the sedimentary archive from Devils Lake has long been acknowledged as a key palaeoenvironmental record (Trowbridge 1917).

Because of its unusual setting (Lytwyn 2010, Attig et al. 2011), Devils Lake has the potential to provide information about very early post-glacial ecosystem development, as well as additional information about the biogeochemical changes coinciding with previously documented climate and vegetation changes. We present geochemical, biological, and geophysical data from a new, ~10 m long sediment core retrieved in February 2012 that describe the evolution of the catchment ecosystem. We chose proxies that complement the detailed pollen record and provide information about sediment sources, organic matter, nutrient cycling, and important terrestrial ecosystem processes like fire. Collectively, these proxies combine to reveal a history of long-term climatic, vegetative and geologic change within this region during the crucial Pleistocene to Holocene transition. Additionally, this record provides further information on the timing and rate of primary succession processes as well as interactions with biotic and climatic drivers during the Holocene.

2. Regional Setting and Study Site

Devils Lake, Sauk County, Wisconsin (43°25.08′N, 89°43.92′W, 294 m asl) lies in a stream-cut, Precambrian quartzite gorge within the Baraboo Hills syncline (Lytwyn 2010), although the presence of sandstone proximal to the current lake levels does suggest that a depression previously existed (Trowbridge 1917). The gorge is constrained by exposed, steep, rocky bluffs on the east, west and south sides (Lillie and Mason 1986) that are up to 150m above the current lake level (Fig. 1). The lake was formed when the northern and southeastern ends of the Devils Lake Gorge were plugged by the Johnstown moraine, deposited at the maximum extent of the Green Bay Lobe. It is likely that Devils Lake became a continually inundated basin by 21,000 cal yr BP but certainly by 18,500 cal yr BP, when OSL ages of sediment deposits suggest the Green Bay Lobe began thinning and retreating (Attig et al. 2011). Independent radiocarbon dating of lacustrine sediments just south of Devils Lake indicates that the position of ice here during the glacial maximum may have been quite prolonged, with the Green Bay Lobe at its maximum position from about 26,400±5,100 cal yt BP to 21,400±3,300 cal yr BP (Carson et al. 2012). Further, there may have been extremely rapid collapse of the Green Bay Lobe after this point as inferred from available and nearby radiocarbon evidence (Maher and Mickelson 1996).

Today the Johnstown moraine at the north end is approximately 20-26 m high (above the water level) and 0.3 km wide, and 25-35 m high and 1 km wide at the southeastern end (Clayton and Attig 1990). Presently, Devils Lake has a maximum water depth of ~14 m and surface area of 153 ha. Two small springs are the only sources of surface inputs, and there are no surface outflows. The lake is dimictic, with turnover occurring in spring and autumn, and exhibits seasonal hypolimnetic anoxia. The geochemistry of Devils Lake is similar to lakes in northern Wisconsin because the Baraboo quartzite outcrops in the watershed, with relatively low acid neutralizing capacity (Herrin et al. 1998).

3. Methods

3.1 Field sampling

A sedimentary sequence of 10.40 m was extracted from the deepest part of Devils Lake in February 2012. The coring location was chosen at the greatest water depth, located using a handheld GPS with reference to previously conducted bathymetric surveys (Fig.

2). Two overlapping piston cores (NICE-EVIL12-1A and NICE-EVIL12-1B) were recovered using a modified Livingstone-type square-rod piston corer (Wright 1967) with staggered starting depths. The overlap ensured that the entire lacustrine sedimentary section was collected despite potential loss from core tube ends and unrecognized gaps between successive sections.

Sediments were extruded from the steel barrel of the corer into acrylonitrile butadiene styrene (ABS) casing, securely wrapped and transported to the LacCore facility and kept in cold storage. The uppermost sediments (first 2 drives) were obtained using the Bolivia modification in which 1.5m polycarbonate core tubes are used. In this case, sediment was not extruded in the field and the polycarbonate tubes were sealed on site. In order to preserve the sediment/water interface of the initial core drive, sodium polyacrylate powder was added to gel overlying water and "fix" these uppermost sediments.

3.2 Sediment description and spectral analysis

Cores were split and immediately imaged, before oxidation of the sediments could occur, using a Geoscan-III line-scanner. Glare was eliminated by the employment of polarizing filters on the camera and light source. Initial core description was undertaken to further document the sedimentary characteristics using a common classification scheme (Schnurrenberger et al. 2003) and the Munsell Soil Color Charts. Mineral identity and sediment composition were assessed by examination under a polarizing microscope using smear slides and the TMI (Tool for Microscopic Identification; Myrbo et al. 2011).

Accurate colour properties were recorded at the imaging stage of sediment documentation. Cores were imaged alongside a standard 24 colour card to allow for necessary calibration. Separate values for red (R), green (G) and blue (B) color intensities were recorded at a resolution of 0.01 cm. All three colour intensities show a similar variance so the mean red, green and blue (RGB) values are discussed here. Except in unusual circumstances (Moy 2002), spectral properties are often controlled by organic content (Nederbragt et al. 2006), with a strong relationship observed between the colour of the sediment and the total organic carbon (TOC) present (Williams et al. 2011).

3.3 Chronology

The sediment chronology was based upon ^{14}C accelerator mass spectrometry (AMS) dating of six organic samples from the sedimentary sequence as well as the sediment-water interface (Table 1). Samples were analysed at the Center for Accelerator Mass Spectroscopy at Lawrence Livermore National Laboratory, U.S.A. Ages were calibrated using the IntCal13 radiocarbon calibration curve (Reimer et al. 2013) and the age model was developed using Bayesian age modeling in the Bacon package in R [Version 2.2] (Blaauw and Christen 2011). A depositional rate of 35 years/cm was used as the prior in the Bacon program. This rate was based upon the previous core from Devils Lake (Grimm et al. 2009) and other records from the region (Goring 2012). Maximum probability age estimates were returned for each 0.5 cm interval. All ages refer to calendar years before present (BP), where present refers to 1950 C.E. As such, the most modern sediments have dates of negative years BP (e.g. -50 year BP = 2000 C.E.). All dates discussed are expressed as calibrated years before present (cal yr BP).

Inspection of the sediment and the results of the AMS dating reveal that there are no hiatuses or breaks in deposition since the accumulation of material began. High confidence in the sediment integrality and the low analytical uncertainly of the ^{14}C ages allowed all dates, except one (CAMS-160885), to be incorporated into the age-depth model. The highest chronological uncertainty is for the lowest portion of the core below 751 cm, the depth of the oldest radiocarbon date. This is where a slow sedimentation rate combined with low quantities of material to obtain ^{14}C ages make it virtually impossible to determine the ages of the oldest sediments. The maximum and minimum ages for the lowest sampled interval of the sediment core (1040 cm) are 33,585 and 23,175 cal y BP. If the age model is extended to the base of the core, the mean age at the lowest sampled interval of the sediment core is 28,056 cal yr BP. Because of this high chronological uncertainty at depth, we use the age model only to a mean age of 18,468 cal yr BP (769 cm), when the range between the maximum and minimum age (95% confidence level, 2σ) is 5546 years. We report our results for the lowest 270 cm of the sediment core on a depth scale. This enables a temporal context for post-maximum ice sheet events and dynamics that were previously untimed but postdate 18,500 cal yr BP (Attig et al. 2011).

To provide the most accurate comparison between the new 2012 core and the previous core obtained by Maher (1982), the chronology developed by Grimm et al. (2009) was recalibrated using the IntCal13 radiocarbon calibration curve (Reimer et al., 2013) and ages calculated by Bayesian age modeling in the Bacon software in R (Blaauw and Christen, 2011).

3.4 Charcoal

Charcoal analysis was conducted at the Palaeoenvironmental Laboratory at Kansas State University following a modified version of the procedure described by (Long et al. 1998). Subsamples (2 cm^3) were taken at contiguous 1-cm intervals for macroscopic charcoal analysis. Sediments were treated with a 10% solution of H_20_2 for 48-72 hours, before being sieved and separated into two size fractions (>250 and 125-249 µm). Samples were then suspended in water on a gridded Petri dish and counted using a binocular microscope at 25-75× magnification. A distinction was made between arboreal (dark, lattice and branched) and non-arboreal (cellular , fibrous) fragments based upon morphology (Jensen et al. 2007). Charcoal morphotypes have been increasingly used to infer fuel sources for past fires, with the ratio of non-arboreal to total charcoal indicating the proportion of woody fuels (Mueller 2014). This ratio ranges from 0 to 1. Low ratios of non-arboreal to total charcoal in sedimentary samples indicate woody fuel sources, while high ratios indicate herbaceous fuel sources such as grasses and forbs.

Charcoal counts were converted into concentration (particles cm^{-1}) and, using the sediment deposition rate, to charcoal accumulation rates (CHAR, particles cm^{-1} a^{-1}). Charcoal data were then separated in background and peak components using the model CharAnalysis Version 1.1 (Higuera et al. 2009). Background CHAR (changes in fuel abundance and composition) is determined using a LOWESS smoother robust to outliers with a 500-year moving window width and these values are then subtracted from the total CHAR for each interval to provided a record of CHAR peaks (multiple closely timed fires). The peaks are tested for significance using a Gaussian distribution, where peak CHAR values that exceed the 95th percentile are then considered statistically significant. Peaks are then screened to eliminate those that resulted from statistically insignificant variations in CHAR (Gavin et al. 2006). If the maximum count in a CHAR peak has a >5% chance of coming from the same Poisson-distribution population as the minimum charcoal count with the proceeding 75 years, then the peak will then be rejected (Higuera et al. 2009).

3.5 Pollen

The primary pollen stratigraphy of the site was established using a sediment core obtained in 1978 and reported in Maher 1982 and Baker et al. 1993. There were 122 samples analysed from this sediment core, making it one of the highest resolution pollen records obtained from North America. The 2012 cores were subsampled (1cm^3) for pollen and spore analysis, and after spiking with a microsphere solution, which allows for the calculation of concentration data, chemical preparation followed standard palynological protocol and was completed at the LacCore facility. Samples were mounted in silicon oil and counted using 400X magnification. A minimum of 300 terrestrial fossil grains were analysed in each sample, except for the heavily degraded samples. The pollen assemblages from samples from the 2012 core match pollen assemblages from the 1978 core, where they overlap. Note that only six new samples were analysed and reported here, all below 711 cm. Because the original pollen stratigraphy and core chronology were so robust, we report here only these six additional samples in the lowest portions of the 2012 core that predate samples from the 1978 core.

Percentage values for pollen grains were calculated relative to the pollen sum as reported by Baker et al. 1982. The percentages for aquatic taxa, spores and algal remains were calculated relative to the pollen sum plus their own abundance.

3.6 Magnetic parameters

Magnetic parameters in lake sediments are sensitive to changes both external and internal environmental conditions. Concentration-dependent parameters, such as χ, ARM, IRM, saturation remanence (M_{rs}), or saturation magnetisation (M_s) reflect the amount of mineral material contained in the sediment. Interparametric ratios such as χ_{ARM}/IRM and M_{rs}/M_s are indicative of magnetic particle grain size, which also reflects climatic and environmental processes.

Volume-normalised magnetic susceptibility (κ) was measured using the Bartington point sensor (MS2E) attached to the automated Geotex MSCL-XYZ logger at the LacCore facility. Measurements of the exposed surface of the split sediment cores were made at a resolution of 0.5 cm. All other magnetic parameters were measured at the Institute for Rock Magnetism at the University of Minnesota. Subsamples were taken at 5 cm intervals. Wet samples with volumes of approximately 5 cm^3 were freeze-dried and measured for the following magnetic parameters: mass-normalised magnetic susceptibility (χ), anhysteretic remanent magnetisation (ARM), isothermal remanent magnetisation (IRM), and hysteresis parameters. χ was measured on a Kappabridge KLY-2 susceptometer operating at a frequency of 920 Hz. Remanence measurements were performed using a 2G superconducting rock magnetometer. A D-Tech 2000 demagnetiser was used for the acquisition of ARM in a 0.1 mT direct field superimposed on an alternating frequency field decaying at a rate of 5 μT per half cycle from a peak value of 200 mT. ARM susceptibility (χ_{ARM}) was calculated by dividing the ARM to the direct field. IRM was imparted using an ASC Scientific IM-10 30 impulse magnetiser, by exposing the samples to a 200 mT direct field. This measurement was repeated to remove any viscous effects. The ARM ratio (χ_{ARM}/IRM) of each sample was computed by normalising the ARM susceptibility to the IRM.

The ferrimagnetic particle assemblage was modeled using a three end-member mixing model based on bulk remanence and hysteresis parameters (Lascu et al. 2010; 2012). The three end members were assigned the names BIO, PED, and LITH, and represent biogenic, pedogenic, and lithogenic ferrimagnetic components, respectively, each with distinct pairs of M_{rs}/M_s and χ_{ARM}/IRM values (Lascu et al. 2010). The BIO end member ratios were set at M_{rs}/M_s = 0.45 and χ_{ARM}/IRM = 2 mm/A, representative of weakly interacting single domain (SD) particles typical of magnetite grains a few tens of nanometers in size produced by magnetotactic bacteria. These grains are an in-lake source of magnetite, and are synthesised intracellularly by the bacteria, which align them in chains. After the death of the microorganism, the magnetite crystals are preserved in the sediment either as intact or partially collapsed chains. The PED end member ratio values were set at M_{rs}/M_s = 0.2 and χ_{ARM}/IRM = 0.01 mm/A, which are representative of i) small pseudo-single domain (PSD) magnetic particles, a few micrometers in size (Lascu et al. 2010), ii) strongly interacting SD particles (Harrison and Lascu, in press), or iii) a mixture thereof. This component is sourced in the catchment soils, where magnetite is precipitated either abiotically or via dissimilatory bacterial iron reduction. In either case the resulting grain size assemblage comprises tight clumps of particles ranging from nanometer- to micrometer-sized. These pedogenic particles typically reach the lake water via overland flow and runoff, with aeolian pathways being a minor contributor. The LITH end member ratio values were set at M_{rs}/M_s = 0.05 and χ_{ARM}/IRM = 0.01 mm/A, which are representative of magnetite particles with an average grain size of a few tens of micrometers. The source of these larger particles is in crystalline or sedimentary bedrock, and transport to the lake is accomplished by streams and/or wind.

3.7 Organic geochemistry

Organic carbon (C) and nitrogen (N) concentrations and standard isotopic ratios ($\delta^{13}C$, $\delta^{15}N$) were measured on dried bulk sediment samples every 10 cm. Although carbonate content in the sediments was known to be very low from previous analyses, there is some carbonate present in the lower portions of the sediment core due to aeolian activity and transport in the region (Grimm et al. 2009). Therefore, inorganic carbon was removed prior to isotopic analysis using acid pretreatment for sedimentary samples below 550 cm. Analyses were conducted at the Stable Isotope Mass Spectrometry Laboratory at Kansas State University and the Central Appalachian Stable Isotope Facility at the University of Maryland following standard procedures for sediment samples. In-house standards calibrated to PeeDee Belemnite ($\delta^{13}C$) and atmospheric N_2 gas ($\delta^{15}N$) were utilised. Analytical error was better than 0.1 ‰ for $\delta^{13}C$ and better than 0.2 ‰ for $\delta^{15}N$. C:N ratio of the bulk sediment was calculated by dividing %C by %N.

In oligotrophic lakes, sedimentary $\delta^{13}C$ is correlated with lake productivity due to algal photosynthetic demand for dissolved carbon dioxide. Under some conditions, microbial processes of organic carbon, particularly by methanogenic bacteria in anoxic conditions, can leave strongly depleted organic C in the sediments (extremely negative $\delta^{13}C$ values; Hollander and Smith. 2001). Sedimentary $\delta^{15}N$ reflects integrated terrestrial and aquatic N cycling processes, with gaseous losses such as denitrification strongly fractionating and leaving enriched N in the system (McLauchlan et al. 2013b). Sedimentary C:N is interpreted as reflecting the source of organic matter, because aquatic and microbial organic matter has a characteristic C:N of 10, while the C:N of terrestrial material is higher than 10 due to the structural C compounds in higher plants (Meyers. 1994; Kaushal and Binford 1999).

4. Results

4.1. Sediment description

The 10.40 m core was dived into six basic sedimentary units on the basis of mineralogy, biotic components seen from smear slides, and general sediment appearance and composition (Fig. 2). Sediment characteristics indicate a variety of large changes in redox conditions, clastic and biogenic sources of sediment, and mineral composition over the entire record. The six lithological units are numbered sequentially from the top of the core (most recent sediments) to the bottom of the core (oldest sediments): Unit 1 (top of core, 0-21 cm) consists of organic and diatomaceous-rich sapropels with pyrite framboids; Unit 2 consists of organic and diatomaceous-rich sapropels; Unit 3 consists of laminated and banded organic and diatomaceous sapropels with vivianite (hydrated iron phosphate) disappearing halfway in the section and diatoms appearing around the same time; Unit 4 consists of large black bands; Unit 5 consists of massive vivianite-rich clayey silt; and Unit 6 (bottom of core) consists of clay and silt-sized quartz with large amounts of opaque particles (likely pyrite, ferrihydrite and hematite). Turbidite layers are present in Unit 6.

The RGB colour values demonstrate a strong relationship between the colour of the sediment and the total organic carbon (TOC) present (Fig. 2). The grey to dark brown transition occurs gradually from *c*. 748 to 691 cm (middle of Unit 5 to top of Unit 4) and is seen in the RGB colour data. The general trajectory of change is a reduction in RGB values from the basal sediments (>48) to the surface-water interface (<15). Within this general trend two marked features are apparent: i) the large dramatic decline in RGB values from ~40 at 748 cm (17,200 cal yr BP) to ~22 by 691 cm (13,000 cal yr BP), and ii) a further sharp decline in RGB values in sediments deposited above 4cm.

Thin laminae are clearly visible in several portions of the core, which in some sections of the sedimentary sequence could represent varves (annual laminations) either due to seasonal biological activity or seasonal physical dynamics such as glacial meltwater patterns.

4.2. Sediment deposition and chronology

Six ^{14}C AMS dates were used to establish the core chronology for the 2012 Devils Lake core (Table 1). The model reveals a mean sedimentation rate of 23.4 years/cm from 0 to 769 cm (Fig. 3). The highest and most consistent sedimentation rates (19.3 yr/cm) occurred during the most recent period of sediment accumulation, from 701 cm depth to the surface water interface (0 cm) (14,100 cal yr BP to modern). This value is consistent with those rates calculated from the previous core, which averaged 22.3 yr/cm between 633 and 0 cm depth (14,100 cal yr BP to modern) (Maher 1982). The difference in rates can be accounted for by the location of 2012 core and effect of sediment focusing in this deeper portion of the lake. Sedimentation rates in the 2012 core slowed during the older portion of the core, with an average sedimentation rate of 74.6 yr/cm from 769 to 701 cm (18,500 to 13,400 cal yr BP).

There is considerable uncertainty about the age of material below 18,500 cal yr BP (769 cm), but if the age model is extended with the average sedimentation rate for the core, the oldest material could be as old as *c*. 28,000 cal yr BP. This would be the oldest lacustrine sedimentary material discovered in this region by approximately 14,000 years. Several lines of evidence indicate that the lowest core material was deposited in a sedimentary sequence and not significantly reworked or altered by the complicated glacial dynamics of this region: i) the high-resolution magnetic susceptibility measurements (κ) show a strong cyclical stratigraphic pattern for the lower portion of the core (Fig. 5), and ii) the lithology exhibits laminations and banding in a stratigraphic manner in the lower portions of the core.

4.3. Charcoal

The oldest sediments are characterised by the lowest total charcoal abundances observed within the entire record (<14 particles cm^{-3}; mean = 1.8 particles cm^{-3}; Fig. 4). These sediments consist of 299 samples analysed between the base of the core and *c*. 17,000 cal yr BP (1040 and 741.5 cm) with 17.7 % of these samples containing no charcoal particles. The ratio of non-arboreal to total charcoal was low during this period (mean = 0.3). A notable exception to this generally low ratio is seen in a short period of higher values occurring between 820 to 842 cm (mean =1.4, *c*. 20,300 to 21,000 cal yr BP). In total 95% of all charcoal particles were identified as being from an arboreal source. Although these sediments have very low charcoal counts, CHAR analysis suggests a small peak (magnitude = 5) at 18,840 cal yr BP.

The number of charcoal particles abruptly increased at *c*. 17,000 cal yr BP (741.5 cm) and remained high until *c*. 11,600 cal yr BP (642.5 cm). The 98 sediment samples analysed during this time period had a mean of 108.6 particles cm^{-3}. In addition, there was a shift in the ratio of non-arboreal to total charcoal to a mean of 0.14, corresponding to an 83% contribution of charcoal particles from arboreal sources. CHAR analysis indicates 14 fire peaks with magnitudes of 5-162.

From *c*. 11,600 to *c*. 10,000 cal yr BP (642.5 to 581.5 cm) charcoal abundance and fire frequency gradually decreased. Total charcoal count averaged 53.4 particles cm^{-3}. This period includes the Younger Dryas (YD) chronozone, regionally characterised by cool and dry conditions, so we assume that the overall reduction in fire activity is a climatic response. Fuel sources shifted to finer fuels, as indicated by a slightly higher proportion of non-arboreal to total charcoal particles during this period (mean = 0.25) compared to previous samples. CHAR analysis indicates 9 fire peaks during this timeframe with magnitudes <20. Notably, this period is punctuated by an initial short peak in total charcoal counts (max 125; mean 84.6 particles cm^{-3}).

After *c*. 10,000 cal yr BP (581.5 cm) fire activity increased with mean total charcoal counts of 135.8 particles cm^{-3} until *c*. 5,500 cal yr BP (357.5 cm). Despite this overall increase in fire activity, the ratio of non-arboreal to total charcoal remained at similar level to the previous period (mean of 0.26) with 71% of all charcoal particles from arboreal sources. However, there is considerable variability in the fuel source fluctuations during this period, with the ratio of non-arboreal to total charcoal pieces ranging from 0 to 0.61. Fourteen fire peaks are suggested by CHAR analysis with magnitudes from 17 to 340. This period corresponds with a time of high abundance of pollen from hardwood tree species such as *Acer*, *Ostrya/Carpinus*, and *Ulmus* (see below).

A dramatic reduction in fire activity is evident between *c*. 5,500 and *c*. 420 cal yr BP (357.5 -19.5 cm; mean total charcoal = 19.6 particles cm^{-3}). During this period of overall reduction in fire intensity, non-arboreal fuel sources contribute a significant volume, with several distinct fire events (e.g. 4542, 4378 and 784 cal yr BP) comprised of 100% non-arboreal charcoal particles. CHAR analysis suggests that the overall peak magnitude of this timeframe is low. However, 6 peak events are identified with magnitudes 24-61.

The uppermost sediments exhibited another sudden increase in the total number of charcoal particles at *c*. 420 cal yr BP (19.5 cm). This transition aligns precisely with the lithological transition to Unit 1. The mean charcoal counts for the 20 samples in this period are 92.3 particles cm^{-3}, with all samples containing > 11 particles cm^{-3}. The ratio of non-arboreal to total charcoal is once again low (mean = 0.04), with over 88% of all charcoal particles being from arboreal sources. CHAR analysis indicates on fire peak at 375 cal yr BP with an extremely high peak magnitude (155). Background CHAR gradually increases to the present day.

4.4. Pollen

The pollen stratigraphy follows some of the same features as the charcoal data, with some key differences (Fig. 4). Three of the new pollen samples from the 2012 core, those below 750 cm, indicate low pollen influx and poor pollen preservation during this section. This is seen as degraded and oxidised grains as well as high spore concentrations relative to pollen concentrations. Below 750 cm, pollen concentrations are all below 15,000 grains/cc sediment. The basal pollen assemblage at 1034 cm has significantly lower percentages of *Picea* pollen (15%) and higher percentages of Poaceae (38%) and *Artemisia* (9%) than samples in the younger part of the core that date to the maximum glacial extent at 18,500 cal yr BP. The new pollen samples indicate that *Picea* was a significant component on the landscape for several thousand years prior to 11,500 cal yr BP. *Picea* pollen percentages reached 60% by at least 18,500 cal yr BP, although its actual vegetation cover is unclear from pollen assemblage data alone.

No obvious stratigraphic change in pollen assemblages is evident at *c*. 17,000 cal yr BP when fires began occurring on the landscape, but the vegetation type appears to have been similar to spruce forest or tundra due to high percentages of *Picea* pollen (over 50%) as well as Poaceae and *Artemisia* pollen types (over 25%). A relatively stable vegetation composition existed at this time, with some minimal adjustment in the relative proportion of *Picea* on the landscape, as documented in pollen assemblage (45 to 60%).

The pre-Holocene pollen record suggests a slight shift in vegetation composition as documented by a sharp and brief (300 year) decline in *Picea* pollen (to <18%; 588cm) that is concomitant with the onset of the YD chronozone (12,900 cal yr BP). *Fraxinus* pollen also exhibits markedly reduced levels (<10%) during a portion of the YD chronozone, between 12,500 and 11,400 cal yr BP.

The remainder of the Holocene pollen record has been described in great detail elsewhere, but we describe a few of the main features here. Some of the classic successional tree genera—*Populus* and *Betula*—began to increase during or immediately after the YD chronozone*.* *Populus* pollen types are first recorded in significant abundance (>15%) from *c*. 13,400 cal yr BP, and *Betula* pollen types are recorded (>10% pollen) from 12,000 cal yr BP. These genera reached their maxima for the sedimentary record at 12,600 and 10,900 cal yr BP (30 and 25%) respectively. The main feature of the early- to late-Holocene pollen record is the relatively high percentage abundances of hardwood taxa (*i.e. Acer*, *Carya*, *Ostrya*, and *Ulmus)* documented between *c*. 10,500 and *c*. 5,500 cal yr BP. During this period these hardwood taxa accounted for between 41-19% (mean = 28%) of all pollen recorded. Following the decline of the hardwood forest pollen abundance at *c*. 5,500 cal yr BP, herbaceous pollen types doubled in average abundance to 11% of the total pollen sum and remained stable until *c*. 420 cal yr BP. *Quercus* pollen percentages remained high (mean 48%), reaching a maximum of 60% at 3,350 cal yr BP. The uppermost sediments feature a distinctive pollen assemblage, most notably expressed by an abrupt increase in the concentration of *Ambrosia* pollen (>30%) from *c*. 420 cal yr BP. These uppermost sediments also document the lowest percentage abundance of *Pinus* pollen for over 11,000 years.

4.5. Magnetic parameters and measurements

From the base of the core (1040 cm) to *c*. 26,000 cal yr BP (1000 cm), magnetic susceptibility (κ) showed high frequency and high amplitude variation (min=38.6 10^{-5} SI, max=65.2 10^{-5} SI) around a mean of 56.3 10^{-5} (Fig. 5). Magnetic susceptibility values then steadily increased to a maximum of 95.2 10^{-5} SI at *c*. 24,000 cal yr BP (936 cm). After reaching the highest values recorded in the entire record, κ values declined until 16,000 cal yr BP in a cyclical saw-toothed pattern with four peaks (at 849 cm, 804 cm, 17,600 cal yr BP and 16,600 cal yr BP). A final distinct peak is recorded in κ values of 35.8 SI 10^{-5} at 14,700 cal yr BP. A gradual decline in κ is observed for the remainder of the record with two notable exceptions: i) a small increase to 5.9 SI 10^{-5} at *c*. 7,600 cal yr BP (480 cm), and ii) a larger spike to 18.4 SI 10^{-5} at *c*. 120 cal yr BP (8 cm) in the uppermost sediments. M_s and IRM show similar trends, albeit at lower resolution. High values for these concentration-dependent parameters are consistent with sustained input of material of glacial origin. The decline in ARM values is much less prominent, signifying that this parameter is not controlled entirely by lithogenic input, but is sensitive to input of finer material from either the terrestrial of aquatic systems.

The ratio χ_{ARM}/IRM ratio documents low values (<0.2 mm/A) and little variability prior to *c*. 12,800 cal yr BP, reflecting an extremely low proportion of fine-grained magnetite (Fig. 5). A marked increase in χ_{ARM}/IRM occurred *c*. 12,800 cal yr BP, concomitant with a change in lithology at the onset of the YD chronozone. This postdates the establishment of terrestrial vegetation and onset of fire. After 12,800 cal yr BP, χ_{ARM}/IRM steadily increased to 0.8 mm/A by 7,300 cal yr BP, before declining to 0.3 mm/A by 4,800 cal yr BP and remaining below 0.6 until 2,400 cal yr BP. A marked increase occurred at this point (> 1 mm/A) before a sudden and brief maximum value at 140 cal yr BP (1.5 mm/A). A reduction in χ_{ARM}/IRM during the EuroAmerican settlement period at the top of the core occurs after this maximum. The M_{rs}/M_s ratio documents similar fluctuations to χ_{ARM}/IRM, except for the first part of the record (>16,000 cal yr BP), where it exhibits more variability, including a significant peak at ~17,000 cal yr BP.

The component analysis of the ferrimagnetic fraction indicates that the predominant magnetic fraction (represented by the LITH and PED end members) is detrital, eroded from catchment soils and bedrock (Fig. 5). The dominant component is LITH, with a mass fraction >0.5 of the magnetic material for most the entire length of the sediment core. Magnetic concentration was highest and grain size largest during the glacial period, typical of increased erosion in the catchment and potentially also input from nearby glacial lakes which occupied the Stienke and Feltz basin (Attig et al. 2011). The most notable pre-Holocene event in the magnetic record occurred at *c.* 17,000 cal yr BP. Synchronous with the onset of fire, a sharp increase in PED and reduction in LITH fractions occur. These magnetic changes are consistent with pedogenic magnetite from the catchment soils being transferred to the lake after fire events.

Throughout much of the Holocene magnetic concentration generally remained constant, as illustrated by M_s, IRM, and κ. The proportion of magnetosomes originating from magnetotactic bacteria (represented by the BIO end member) increased immediately after deglaciation, as detrital flux decreased and biological productivity increased. During the mid-Holocene the BIO fraction decreased due to sustained detrital fluxes possibly of aeolian origin (McLauchlan et al., 2013a). At 2,400 cal yr BP, a sudden increase in the fraction of BIO occured, which is linked to a reduced influx of detrital grains. Magnetic grain size and concentration increased again in the most recent part of the record, likely due to anthropogenic influence in the region including agriculture-related erosion.

4.6. Carbon and nitrogen measurements

Organic matter concentration of the basal sediments was extremely low, indicating very low or no deposition of organic material. The most obvious stratigraphic change in the organic geochemical record is a regular and prolonged increase in sedimentary organic matter concentration that began *c*. 17,000 cal yr BP and continued until *c*. 12,000 cal yr BP (Fig. 6). During this 5,000 year period, nitrogen (N) concentration increased from 0.14 to 0.84 % and carbon (C) concentration increased from 0.8 to 8.9%. This sudden increase in organic matter close to the beginning of ecosystem development was suggested by other proxies such as spectral analysis and lithology.

This organic matter could be derived from increases in terrestrial primary productivity, lacustrine productivity, or both. There is a clear shift from aquatic or microbial to terrestrial sources of organic matter in the record supported by the C and N data. Sedimentary C:N ratios change from ~5 in basal sediment to >10 by 12,000 cal yr BP. The increase in bulk C:N to a ratio greater than 10 must reflect at least some organic matter contribution from increased terrestrial primary productivity. The contribution of aquatic productivity is more difficult to discern as the interpretation of sedimentary $\delta^{13}C$ cannot simply be correlated with lake productivity, due to extremely negative values (<-26‰). Sedimentary $\delta^{13}C$ was actually declining at the same time as the increases in organic matter concentrations of both C and N, likely indicating increased anoxia due to the deep lake level, relative lack of mixing, and formation of Devils Lake as an isolated basin. The lowest values of sedimentary $\delta^{13}C$ correspond with the black banding in lithological Unit 4 due to reduced iron (14,300 to 12,800 cal yr BP). The trajectory of increasing C and N concentrations seems not to have been affected by this period of anoxia.

Bulk sedimentary $\delta^{15}N$ does not demonstrate much variation across the 17,000 to 12,000 cal yr BP transition zone with the other geochemical proxies, rather continuing to exhibit similar temporal dynamics from the late-Pleistocene towards the Holocene transition. Bulk sedimentary $\delta^{15}N$ integrates a variety of nutrient cycling processes in terrestrial and aquatic habitats, often predominantly reflecting loss of inorganic N to the atmosphere through denitrification. The redox conditions and nutrient status of the lake seem to be dynamic but were not directionally changing during most of the sedimentary record.

A period of slightly elevated $\delta^{15}N$ exists from 12,700 to 5,600 cal yr BP, contemporaneous with lithological Unit 3. While the timing of more recent decline in $\delta^{15}N$ of this period can be closely associated with the decrease in hardwood taxa and total charcoal count (see above) as well as the lithological transition from Unit 3 to Unit 2, the increase is only loosely linked to changes in pollen assemblage (i.e. *Ulmus* and *Betula*). There is one additional geochemical change during the Holocene: a reduction in OM concentration (both %C and %N), a decline in C:N, and a decline in $\delta^{15}N$ around 7,500 cal yr BP. A sudden decline in sedimentary $\delta^{15}N$ at the top of the core around after 130 cal yr BP (8 cm) is likely due to agricultural transformation of the region. Reductions in %C and %N predate this decline in $\delta^{15}N$ (by 200 years) but strongly indicate increased clastic input during this time period, consistent with erosional inputs from increased agriculture.

5. Discussion

5.1. Reconstruction of environments from pre-glacial maximum

The oldest portion of the sedimentary record (>18,500 cal yr BP) is in some ways the most intriguing, as regional lacustrine sedimentary records of this duration are extremely scarce. Although the precise chronology remains unknown, the basal sediments of Devils Lake could be 28,000 years old, which would revolutionise the temporal resolution of glacial dynamics in this region. Recent work suggests that regional lake formation could have been underway at this time (Carson et al. 2012). We do know that the ice sheet was very close to the site during much of this time period (within tens of km) and must have been adjacent to the lake at the time of terminal moraine formation, and thus maximum ice sheet extent (Attig et al. 2011). During this time there was virtually no organic matter input to lake (either terrestrial or aquatic), as documented by the extremely low sedimentary %C and RGB values. Interpretation of the vegetation at this time is not straightforward: the pollen percentages alone indicate a spruce tundra but the low concentrations and poor pollen preservation indicate the potential for a tundra with only a few sparse trees or some bare soil surface with little vegetation cover. An increasing number of cryptic refugia have recently been discovered in high latitude locations thought to have been ice-covered or otherwise climatically unsuitable for vegetation growth, including Europe (Parducci et al. 2012) and North America (Petit et al. 2008). The spruce pollen in the Devils Lake record during pre-glacial maximum times may indicate spruce trees growing closer to the glacial margin of the Laurentide Ice sheet than previously supposed, perhaps on the highlands either side of the current lake basin. There is one continuous and well-dated pollen record from this time period, approximately 550 km to the south of Devils Lake (at Pittsburg Basin in central Illinois), and it contains records of several recurrences of *Pinus* and *Picea* forests during glacial times (Teed 2000).

The relative vegetation stability (*Picea* pollen percentages of 45 to 60%) occurred during one of the most dynamic portions of the entire record regarding climatic and geomorphological change, and therefore does not support the idea of a primary successional sequence, even a very slow one that took place over a timeframe of 2,000 years. There is not much evidence for primary succession that was hypothesised to occur in the region as a blank landscape was colonised first by tundra vegetation, then spruce trees.

Whatever the vegetation composition at Devils Lake during the early postglacial period, there were no fires on the landscape at this time. To our knowledge, there are no other charcoal records from this time period and region, making this site an important data point indicating lack of fire at this time for regional and global fire reconstructions (Power et al. 2010; Marlon et al. 2009). The charcoal record from Pittsburgh Basin indicates relatively low fire frequency during glacial times, despite the presence of glacial *Picea* forests (Teed 2000). The magnetic parameters at Devils Lake indicate high erosion rates supplying significant amounts of clastic material to the lake, but sedimentation rate is difficult to estimate due to the chronological uncertainty in this section of the core. This material is derived from either glacial-periglacial environments or soils, and was likely transported to the lake *via* riverine, meltwater, or aeolian pathways. The apparent cyclicity in the κ data hints at a possible link with climate records from oxygen isotopes preserved in speleothems from Iowa and Missouri (Dorale et al. 2010). However, it is likely that these sedimentary magnetic fluctuations reflect more local climatic controls or localised ice sheet dynamics (marginal collapses, melt water release events), as they do not precisely match dynamics seen in the Greenland ice cores (Blaauw et al. 2010).

5.2. Biotic and abiotic interactions during ecosystem development

5.2.a. Post glacial maximum

While the timing of local ice sheet maximum extent is difficult to determine without large dating errors, the glacial ice at the Devils Lake site had begun to thin and retreat at *c.* 18,500 cal yr BP (Attig et al. 2011, Carson et al. 2012). The sedimentary succession at Devils Lake uniquely records several key events which occurred during and after this retreat, although somewhat asynchronously.

The abrupt onset of fire at 17,000 cal yr BP is a strong feature of the Devils Lake record that is not currently associated with a known mechanism. The onset of fire cannot be associated with an obvious vegetation change, as pollen assemblages indicate the presence of a spruce tundra or forest both immediately before and after 17,000 cal yr BP. Sites several hundred kilometers to the south indicate more productive spruce forest than likely existed at Devils Lake, but a similar abrupt onset of fire. A fire regime initiated *c*. 10,500 cal yr BP (in Indiana) and *c*. 15,500 cal yr BP (in Ohio) when charcoal morphotypes indicate woody fuel sources (Gill et al. 2009, Gill et al. 2012). Whatever the trigger for the onset of fire at Devils Lake, the impact was a brief period of high transfer of soil-derived particles, as evidenced by the magnetic component PED.

The second main change in ecosystem development was the start of an increase in organic matter concentration within the lake sediments that also began at c.17,000 cal yr BP. This steady increase in organic matter occurred over a 5000 year period between *c*. 17,000 cal yr BP and *c*. 12,000 cal yr BP. Other sites, such as a high-altitude mountain lake in Switzerland (Thevenon et al. 2012), do not exhibit such a clear and prolonged rate of organic matter accumulation. Although large changes in fire and organic matter input early in ecosystem development are indications of strong biotic control, there is also evidence that some aspects of ecosystem development were strongly abiotically controlled, specifically lake processes and productivity. In particular, there was a hypothesised anoxic period in lithologic Unit 4 (*c*. 14,300 - *c*. 12,800 cal yr BP) due to the presence of cold, deep, stratified lake water.

5.2.b. Younger Dryas

The YD chronozone (12,800-11,500 cal yr BP) can be thought of as a climate perturbation to the trajectory of ecosystem development. This period was cool and dry in the region, which seems to be supported with well-dated synoptic studies (Shuman et al. 2002, Grimm et al. 2009). At Devils Lake the main expression of the YD was a brief decline in *Picea* pollen and a concomitant increase in *Populus* pollen percentages. There was a slight reduction in fire activity possibly due to increased aridity. Brief droughts have affected fire activity in spruce forests and tundra in Alaskan ecosystems (Hu et al. 2010). Arid conditions have been demonstrated throughout the midcontinent during the YD, with steep environmental gradients ranging from a C4-rich prairie in southwestern Missouri to spruce forests in Iowa, Illinois, and Ohio (Dorale et al. 2010) as well as the Devils Lake site farther to the north.

Although the terrestrial ecosystem had been functioning for several thousand years, at least with some vegetation on the landscape, aquatic productivity did not become significant until 12,800 cal yr BP when anoxic conditions ceased at the beginning of the YD—this is seen as an increase in $\delta^{13}C$ values, an increase in organic matter C:N, and the first appearance of diatoms in the sediment core. All of these proxies taken together indicate increased algal productivity. This increase in productivity may have been triggered by a combination of climate change, the lake becoming shallow and more mixed, and the establishment of moraines in their final configuration. However, despite this one significant ecosystem shift during the YD, this site is really not the strongest expression of the YD chronozone. What is apparent is that no single proxy adequately brackets the YD chronozone, with some responding during the onset, others adjusting at the termination, and many demonstrating no shift whatsoever.

5.2.c. Holocene

The main change during the Holocene was an increase in fire activity for a 6,000 year period of hardwood forest (c.11,000 to 5,000 cal yr BP). This is a rare type of fire regime for this vegetation structure, as today modern hardwood forests often exhibit no fire occurrence (Nowacki and Abrams 2008); therefore the potential fire regimes of hardwood forests have not received much attention in sedimentary palaeorecords. Although hardwood forest fire regimes are not well-understood, fire reconstructions of hardwood forests in central Minnesota indicate there has been significant charcoal influx from past hardwood forests primarily consisting of *Acer*, *Ostrya-Carpinus*, *Ulmus* and other hardwood tree species, suggesting that ground fires were more common than assumed (Umbanhowar 2004). The increases in fire frequency and possibly severity during the hardwood period at Devils Lake appear to be driven by climate and mediated through changes in vegetation composition and structure. There are also unanswered questions about the degree of regional synchrony in fire regimes (Marlon et al. 2009), with sites in *Quercus*-dominated forests to the east demonstrating highly individualistic fire patterns throughout the Holocene (Mueller 2014).

Nutrient cycling appears to have been dynamic throughout the Holocene but did not demonstrate much or any directional change over time. If we assume that the mid-Holocene was warm at this site, as interpreted by the original analysts (Baker et al. 1992), there should be some ecosystem-level consequences of this warming. A study of 20 lakes to the west in Minnesota indicated that climate change during the past ~1000 years did have regional effects on lake ecosystems (some with hardwood-forested catchments) including changes in sedimentary C:N, organic matter concentration, and $\delta^{15}N$ with warming, but that among-lake variability was high, reflecting the importance of local factors (Umbanhowar et al. 2011). This confirms the idea that the lake is filtering environmental changes in the catchment (Olsen et al. 2013). In any case, there does not seem to be a strong case for expression of the mid-Holocene Warm Period in pollen, charcoal, or other proxies.

One notable change during the mid-Holocene at Devils Lake was the lithological change at c. 6,000 cal yr BP. This change is associated with a decline in $\delta^{15}N$, decline in hardwood pollen types, decline in total charcoal, and a slight increase in non-arboreal charcoal morphotypes. It is also approximately timed with a decline in the proportion of BIO and an increase in the LITH fraction. Prior to this point, sedimentary $\delta^{15}N$ seemed unaffected by changes in terrestrial ecosystem processes such as pollen and charcoal.

After this point, sedimentary $\delta^{15}N$ seems linked with these proxies, indicating a switch in control.

Magnetic concentration-dependent parameters (κ, IRM, M_s) indicate a steady decline in the mass fraction of ferrimagnetic material, which decreases by more than an order of magnitude from the LGM to the beginning of the Holocene, after which the concentration remains relatively constant except for very recent times. The decline in several magnetic parameters, including C_{ferri}, χ, κ, and M_s, indicates reduced terrestrial input over time and may be a consequence of landscape stabilisation. A gradual reduction in terrestrial inputs over the history of ecosystem development was also seen in Deming Lake, Minnesota (McLauchlan et al. 2013a). This trajectory of gradual dystrophication has been proposed as a consequence of reduced material flux over time (Leavitt et al. 2009) and has also been seen in an oligotrophic lake in Scotland (Oldfield et al. 2010). There was a reduction in the fraction of BIO from *c*. 5,000 to 3,000 cal yr BP, then an increase to the highest levels in the record, corresponding to the most eutrophic conditions observed in the record, just prior to the period of strong anthropogenic influence. This increase in the proportion of magnetosomes after 3,000 cal yr BP may indicate either reduced erosion rates in the catchment, or high rates of magnetosome production in the lake. The increase in ARM values and %N at the same time supports the latter scenario, suggesting an increase in nutrient delivery to the lake water during a period of warm/humid climatic conditions.

The final step of ecosystem development at this site involves the recent imprint of anthropogenic activities. The Devils Lake sediment core, like many other sites, records a set of commonly-observed changes seen in the Midwestern region due to Euro-American settlement and land use change beginning in the 19th century. Along with the ubiquitous *Ambrosia* rise and increase in fire activity seen in much of North America (Foster et al. 1998), there are clear increases in sedimentary input reflected in lithological change and magnetic parameters. There is a decline in organic matter concentrations with increased clastic inputs due to increased erosion, and an abrupt decline in sedimentary $\delta^{15}N$. The decline in sedimentary $\delta^{15}N$ has been observed in several, but not all, sediment cores from North America and is generally attributed to increased fertiliser input although other mechanisms are possible (Holtgrieve et al. 2011). Interestingly, the magnitude of the modern anthropogenic changes is not as large as some of the earlier changes, which contradicts many records of geochemical and ecological change where the anthropogenic period is unprecedented during the Holocene (Engstrom and Rose 2013).

5.3. Linking palaeorecords of ecosystem development with chronosequences

The nutrient dynamics of these changes in ecosystem properties and landscape evolution are still relatively unexplored. The sedimentary $\delta^{15}N$ record at Devils Lake exhibits unexplained variation, with the intriguing possibility of a change in controls on nutrient dynamics from climatic factors to terrestrial ecosystem processes at *c*. 6,000 cal yr BP. Further investigation at higher temporal resolution would be required to test this hypothesis. From modern landscapes with rocks of different ages, there are some estimates of weathering rates, mineral transformations, and indications of interactions between vegetation and the lithosphere (Chadwick et al. 1999, Hahm et al. 2014). Again, several different absolute rates have been measured, leading to difficulties in identifying drivers and generalising the processes (Walker et al. 2010). Additionally, it is difficult to locate an area with enough variables under control, such that only six chronosequences suitable for detailed geochemical study have been identified on Earth (Wardle et al. 2004). While there is great potential to further understand long-term ecosystem development through further study of chronosequences (Wardle et al. 2012), we suggest here a complementary approach. There is also the potential to use sedimentary sequences to assess the absolute rates of these processes as well as interactions with climate changes and biotic changes observed during the Holocene. One good example of this approach is a study at Lake Sägistalsee in the Bernese Alps in Switzerland which investigated rates of carbonate and silicate weathering over 9,000 years of ecosystem development, finding a significant influence of vegetation and human activities on these processes (Koinig et al. 2003).

6. Conclusions

This record demonstrates two important new concepts about primary succession. First, the newly-deglaciated landscape was not a blank slate for plants to colonise, rather it retained the imprint of glacial dynamics that set the stage and possibly the trajectory for ecosystem change at this site. Quantities of glacial meltwater, position of ice, unique bedrock configuration, aeolian input, surviving vegetation, and till composition all contributed to the palaeorecord at Devils Lake. Second, primary succession did not consist of a series of events acting perfectly in synchrony, or even sequentially. Rather several different processes were initiated at different times and at different rates, driven by independent factors such as geomorphic change, climate conditions, and biotic factors both in the terrestrial and aquatic system. While these could be interpreted as individualistic proxy responses, it is more useful to think of these as linked processes capturing different signals from the system. Further, interactions between the climate and terrestrial system, and inputs from terrestrial to aquatic systems, combined to produce the particular pattern of palaeoenvironmental change documented at this site throughout the Holocene. While embedded in regional setting, Devils Lake provides a unique and very long record of ecosystem change through perhaps as much as the past 28,000 years.

Acknowledgments

This research was funded by a NSF grant to KKM (BCS-0955225). The LacCore facility is supported by NSF IF-0949962. EMM was funded by NSF REU EAR-1062775. We would like to thank Louis Maher and Eric Grimm for permission to use the previously established pollen data set and chronology. Kristina Brady, Colin Long and Stacey Henck provided field assistance, Scott McConaghy assisted with charcoal data collection, and

Julie Commerford and Kyleen Kelly analysed the new pollen samples. Troy Ocheltree and Robin Paulman performed the isotopic analysis.

Table 1. Radiocarbon dates and errors for sediment from Devils Lake, Wisconsin, U.S.A. Radiocarbon analyses were conducted at the Center for Accelerator Mass Spectrometry (CAMS) at Lawrence Livermore National Laboratory.

Lab code	Composite depth below the sediment-water interface (cm)	Description	^{14}C age (years BP)	Error (years)	Cal yr BP ±1σ
CAMS-160886	152	pollen	2990	30	3195 ± 126
CAMS-160879	360	charcoal	4740	100	5395 ± 310.5
CAMS-160878	536.5	charcoal	7810	110	8696 ± 282
CAMS-165605	650.5	pollen	10200	40	11915.5 ± 160.5
CAMS-165606	701	pollen	11655	35	13496.5 ± 70.5
CAMS-165607	751.5	pollen	15780	430	19194.5 ± 910.5
CAMS-160885		pollen	>22800		not used due to high uncertainty because of insufficient carbon

Figure captions

Figure 1. Location of Devils Lake, Wisconsin, USA in the Baraboo Hills region of the upper Midwestern U.S. Bathymetry of Devils Lake. Coring site from 2012 is shown along with the coring site from 1978 reported by Baker et al. (1993) A digital elevation model of the Devils Lake catchment along with maximum extent of Green Bay Lobe of the Laurentide Ice Sheet at ~ 18.5 kya is shown (Attig et al. 2011). Contour lines at 50 m intervals.

Figure 2. Bayesian age-depth model performed with Bacon (Blaauw and Christen, 2011) for the Devils Lake sediment core. The upper left panel shows the iteration history, the upper middle panel shows the prior (green line) and posterior (gray area) of the sediment accumulation rate (yr/cm), and the upper right panel shows the prior (green line) and posterior (gray area) of the memory (1 cm autocorrelation strength). The bottom panel shows the age-depth models with uncertainties. The solid red line is the weighted averages of all possible chronologies. Associated uncertainties are represented by the grayscale and confidence intervals (dotted black lines).

Figure 3. Details of the sediment core lithology including spectral analysis of core colour intensities (mean RGB values), the stratigraphy of the six identified units (see main text for description) and a composite image of the entire sediment core. Images of smear slides from five of the six lithological units are also shown; Unit 1, organic and diatomaceous-rich sapropels with pyrite framboids. Unit 3, diatomaceous sapropels with vivianite. Units 4 and 5, massive vivianite-rich clayey silt. Unit 6, clay and silt-sized quartz with large quantities of pyrite, ferrihydrite and hematite.

Figure 4. Terrestrial vegetation dynamics represented in pollen and charcoal from Devils Lake sediment. Red lines indicate transitions among the six lithologic units. Pollen percentages of selected pollen taxa, total charcoal counts, ratio of non-arboreal morphotype charcoal pieces: total charcoal pieces, and CHAR output indicating fire episodes per 1000 yr (crosses) and peak magnitudes (line) (Higuera et al. 2009, Higuera et al. 2010). Pollen data reported in Baker et al. (1993) are shown in colour, with new pollen samples represented as black bars. Red lines indicate transitions among the six lithologic units.

Figure 5. Magnetic parameters and measurements. Red lines indicate transitions among the six lithologic units. Measurements include: M_s - saturation magnetization (total ferrimagentic concentration proxy), ARM - anhysteretic remanent magnetisation (sensitive to the concentration of fine-grained remanence-carrying particles), IRM - isothermal remanent magnetisation (a measure of the concentration of all remanence-carrying grains), χ_{ARM}/IRM (indicative of magnetic grain size, as well as magnetostatic interactions between SD grains), and M_{rs}/M_s (magnetic grain size proxy). Cumulative plot of the biogenic, pedogenic, and lithogenic ferrimagnetic particle grain size components, calculated using a three end-member mixing model based on remanence

and hysteresis parameters. High resolution volume-normalised magnetic susceptibility (κ).

Figure 6. Organic geochemical proxies: %C, %N, C:N, $\delta^{13}C$, and $\delta^{15}N$. Red lines indicate transitions among the six lithologic units. All samples below 9080 cal yr BP (550 cm) were acidified to remove carbonates.

References

Attig, J. W., P. R. Hanson, J. E. Rawling, A. R. Young, and E. C. Carson. 2011. Optical ages indicate the southwestern margin of the Green Bay Lobe in Wisconsin, USA, was at its maximum extent until about 18,500 years ago. Geomorphology 130:384-390.

Baker, R. G., L. J. Maher, C. Chumbley, A., and K. L. Van Zant. 1992. Patterns of Holocene environmental change in the midwestern United States. Quaternary Research 37:379-389.

Blaauw, M., and J. A. Christen. 2011. Flexible paleoclimate age-depth models using an autoregressive gamma process. Bayesian Analysis 6:457-474.

Blaauw, M., B. Wohlfarth, J. A. Christen, L. Ampel, D. Veres, K. A. Hughen, F. Preusser, and A. Svensson. 2010. Were last glacial climate events simultaneous between Greenland and France? A quantitative comparison using non-tuned chronologies. Journal of Quaternary Science 25:387-394.

Carson, E. C., P. R. Hanson, J. W. Attig, and A. R. Young. 2012. Numeric control on the late-glacial chronology of the southern Laurentide Ice Sheet derived from ice-proximal lacustrine deposits. Quaternary Research 78:583-589.

Chadwick, O. A., L. A. Derry, P. M. Vitousek, B. J. Huebert, and L. O. Hedin. 1999. Changing sources of nutrients during four million years of ecosystem development. Nature 397:491-497.

Clayton, L., and J. W. Attig. 1990. Geology of Sauk County, Wisconsin: Wisconsin Geological and Natural History Survey Information Circular 67.

Dorale, J. A., L. A. Wozniak, E. A. Bettis, S. J. Carpenter, R. D. Mandel, E. R. Hajic, H. Lopinot, and J. H. Ray. 2010. Isotopic evidence for Younger Dryas aridity in the North American midcontinent. Geology 38:519-522.

Engstrom, D. R., S. C. Fritz, J. E. Almendinger, and S. Juggins. 2000. Chemical and biological trends during lake evolution in recently deglaciated terrain. Nature 408:161-166.

Engstrom, D. R., and N. L. Rose. 2013. A whole-basin mass-balance approach to paleolimnology. Journal of Palaeolimnology.

Finkenbinder, M. S., M. B. Abbott, M. E. Edwards, C. T. Langdon, B. A. Steinman, and B. P. Finney. 2014. A 31,000 year record of paleoenvironmental and lake-level change from Harding Lake, Alaska, USA. Quaternary Science Reviews 87:98-113.

Foster, D. R., G. Motzkin, and B. Slater. 1998. Land-use history as long-term broad-scale disturbance: regional forest dynamics in central New England. Ecosystems 1:96-119.

Gavin, D. G., F. S. Hu, K. Lertzman, and P. Corbett. 2006. Weak climatic control of stand-scale fire history during the late Holocene. Ecology 87:1722-1732.

Gill, J. L., J. W. Williams, S. T. Jackson, J. P. Donnelly, and G. C. Schellinger. 2012. Climatic and megaherbivory controls on late-glacial vegetation dynamics: a new, high-resolution, multi-proxy record from Silver Lake, Ohio. Quaternary Science Reviews 34:66-80.

Gill, J. L., J. W. Williams, S. T. Jackson, K. B. Lininger, and G. S. Robinson. 2009. Pleistocene Megafaunal Collapse, Novel Plant Communities, and Enhanced Fire Regimes in North America. Science 326:1100-1103.

Goring, S., J.W. Williams, J.L. Blois, S.T. Jackson, C.J. Paciorek, R.K. Booth, J.R. Marlon, M. Blaauw, J.A. Christen. 2012. Deposition times in the northeastern United States during the Holocene: establishing valid priors for Bayesian age models. Quaternary Science Reviews 48:54-60.

Grimm, E. C., L. J. Maher, and D. M. Nelson. 2009. The magnitude of error in conventional bulk-sediment radiocarbon dates from central North America. Quaternary Research 72:301-308.

Hahm, W. J., C. S. Riebe, C. E. Lukens, and S. Araki. 2014. Bedrock composition regulates mountain ecosystems and landscape evolution. Proceedings of the National Academy of Sciences of the United States of America 111:3338-3343.

Harrison, R. J., and Lascu, I. FORCulator: A micromagnetic tool for simulating first-order reversal curve diagrams. Geochemistry Geophysics Geosystems. (In press).

Herrin, R. T., R. C. Lathrop, P. R. Gorski, and A. W. Andren. 1998. Hypolimnetic methylmercury and its uptake by plankton during fall destratification: A key entry point of mercury into lake food chains? Limnology and Oceanography 43:1476-1486.

Higuera, P. E., L. B. Brubaker, P. M. Anderson, F. S. Hu, and T. A. Brown. 2009. Vegetation mediated the impacts of postglacial climate change on fire regimes in the south-central Brooks Range, Alaska. Ecological Monographs 79:201-219.

Higuera, P. E., D. G. Gavin, P. J. Bartlein, and D. J. Hallett. 2010. Peak detection in sediment-charcoal records: impacts of alternative data analysis methods on fire-history interpretations. International Journal of Wildland Fire 19:669- 1014.

Hollander, D. J., and M. A. Smith. 2001. Microbially mediated carbon cycling as a control on the delta C-13 of sedimentary carbon in eutrophic Lake Mendota (USA): New models for interpreting isotopic excursions in the sedimentary record. Geochimica Et Cosmochimica Acta 65:4321-4337.

Holtgrieve, G. W., D. E. Schindler, W. O. Hobbs, P. R. Leavitt, E. J. Ward, L. Bunting, G. Chen, B. P. Finney, I. Gregory-Eaves, S. Holmgren, M. J. Lisac, P. J. Lisi, K. Nydick, L. A. Rogers, J. E. Saros, D. T. Selbie, M. D. Shapley, P. B. Walsh, and A. P. Wolfe. 2011. A Coherent Signature of Anthropogenic Nitrogen Deposition to Remote Watersheds of the Northern Hemisphere. Science 334:1545-1548.

Hu, F. S., P. E. Higuera, J. E. Walsh, W. L. Chapman, P. A. Duffy, L. B. Brubaker, and M. L. Chipman. 2010. Tundra burning in Alaska: linkages to climatic change and sea-ice retreat. Journal of Geophysical Research-Biogeosciences 115:G04002.

Jenny, H. 1941. Factors of soil formation: a system of quantitative pedology. McGraw Hill, New York, USA.

Jensen, K., E. A. Lynch, R. Calcote, and S. C. Hotchkiss. 2007. Interpretation of charcoal morphotypes in sediments from Ferry Lake, Wisconsin, USA: do different plant fuel sources produce distinctive charcoal morphotypes? Holocene 17:907-915.

Kaushal, S., and M. W. Binford. 1999. Relationship between C:N ratios of lake sediments, organic matter sources, and historical deforestation in Lake Pleasant, Massachusetts, USA. Journal of Paleolimnology 22:439-442.

Koinig, K. A., W. Shotyk, A. F. Lotter, C. Ohlendorf, and M. Sturm. 2003. 9000 years of geochemical evolution of lithogenic major and trace elements in the sediment of an alpine lake - the role of climate, vegetation, and land-use history. Journal of Paleolimnology 30:307-320.

Leavitt, P. R., S. C. Fritz, N. J. Anderson, P. A. Baker, T. Blenckner, L. Bunting, J. Catalan, D. J. Conley, W. O. Hobbs, E. Jeppesen, A. Korhola, S. McGowan, K. Ruhland, J. A. Rusak, G. L. Simpson, N. Solovieva, and J. Werne. 2009. Paleolimnological evidence of the effects on lakes of energy and mass transfer from climate and humans. Limnology and Oceanography 54:2330-2348.

Lillie, R. A., and J. W. Mason. 1986. Historical changes in water quality and biota of Devils Lake, Sauk County 1866-1985. Transactions of the Wisconsin Academy of Sciences, Arts and Letters 74:81-104.

Long, C. J., C. Whitlock, P. J. Bartlein, and S. H. Millspaugh. 1998. A 9000-year fire history from the Oregon Coast Range, based on a high-resolution charcoal study. Canadian Journal of Forest Research 28:774-787.

Lytwyn, J. 2010. Remote sensing and GIS investigation of glacial features in the region of Devils Lake State Park, South Central Wisconsin, USA. Geomorphology 123:46-60.

Maher, L. J. 1982. The palynology of Devils Lake, Sauk County, WI. . Quaternary History of the Driftless Area. University of Wisconsin Extension, Geological and Natural History Survey, Madison, Wisconsin.

Maher, L. J., and D. M. Mickelson. 1996. Palynological and Radiocarbon Evidence for Deglaciation Events in the Green Bay Lobe, Wisconsin. Quaternary Research 46:251–259.

Marlon, J. R., P. J. Bartlein, M. K. Walsh, S. P. Harrison, K. J. Brown, M. E. Edwards, P. E. Higuera, M. J. Power, R. S. Anderson, C. Briles, A. Brunelle, C. Carcaillet, M. Daniels, F. S. Hu, M. Lavoie, C. Long, T. Minckley, P. J. H. Richard, A. C. Scott, D. S. Shafer, W. Tinner, C. E. Umbanhowar, and C. Whitlock. 2009. Wildfire responses to abrupt climate change in North America. Proceedings of the National Academy of Sciences of the United States of America 106:2519-2524.

McLauchlan, K. K., I. Lascu, A. Myrbo, and P. R. Leavitt. 2013a. Variable ecosystem response to climate change during the Holocene in northern Minnesota, USA. . Geological Society of America Bulletin 125:445–452.

McLauchlan, K. K., J. J. Williams, and D. R. Engstrom. 2013b. Nutrient cycling in the palaeorecord: Fluxes from terrestrial to aquatic ecosystems. Holocene 23:1635–1643.

Meyers, P. A. (1994). Preservation of elemental and isotopic source identification of sedimentary organic matter. Chemical Geology, 114(3), 289-302.

Milner, A. M., C. L. Fastie, I. Chapin F S, D. R. Engstrom, and L. C. Sharman. 2007. Interactions and linkages among ecosystems during landscape evolution. Bioscience 57:237-247.

Mourier, B., J. Poulenard, C. Carcaillet, and D. Williamson. 2010. Soil evolution and subalpine ecosystem changes in the French Alps inferred from geochemical analysis of lacustrine sediments. Journal of Paleolimnology 44:571-587.

Moy, C. M., Seltzer, G.O., Rodbell, D.T., Anderson, D.M. 2002. Variability of El Niño/ Southern Oscillation activity at millennial timescales during the Holocene epoch. Nature 420:162–165.

Mueller, J. R., C. J. Long, J. J. Williams, A. Nurse, and K. K. McLauchlan. . 2014. The relative controls on forest fires and fuel source fluctuations in the Holocene deciduous forests of southern Wisconsin, USA. Journal of Quaternary Science 29:561-569.

Myrbo, A., Morrison, A., and McEwan, R. (2011). Tool for Microscopic Identification (TMI). http://tmi.laccore.umn.edu. Accessed on 11 November 2014

Nederbragt, A. J., R. B. Dunbar, A. T. Osborn, A. Palmer, J. W. Thurow, and T. Wagner. 2006. Sediment colour analysis from digital images and correlation with sediment composition. Pages 113-128 Geological Society, London, Special Publications.

Nowacki, G. J., and M. D. Abrams. 2008. The demise of fire and "Mesophication" of forests in the eastern United States. Bioscience 58:123-138.

Oldfield, F., R. W. Battarbee, J. F. Boyle, N. G. Cameron, B. Davis, R. P. Evershed, A. D. McGovern, V. Jones, R. Thompson, and R. Walker. 2010. Terrestrial and aquatic ecosystem responses to late Holocene climate change recorded in the sediments of Lochan Uaine, Cairngorms, Scotland. Quaternary Science Reviews 29:1040-1054.

Olsen, J., N. J. Anderson, and M. J. Leng. 2013. Limnological controls on stable isotope records of late-Holocene palaeoenvironment change in SW Greenland: a paired lake study. Quaternary Science Reviews 66:85-95.

Parducci, L., T. Jorgensen, M. M. Tollefsrud, E. Elverland, T. Alm, S. L. Fontana, K. D. Bennett, J. Haile, I. Matetovici, Y. Suyama, M. E. Edwards, K. Andersen, M. Rasmussen, S. Boessenkool, E. Coissac, C. Brochmann, P. Taberlet, M. Houmark-Nielsen, N. K. Larsen, L. Orlando, M. T. P. Gilbert, K. H. Kjaer, I. G. Alsos, and E. Willerslev. 2012. Glacial Survival of Boreal Trees in Northern Scandinavia. Science 335:1083-1086.

Petit, R. J., F. S. Hu, and C. W. Dick. 2008. Forests of the past: A window to future changes. Science 320:1450-1452.

Power, M. J., J. R. Marlon, P. J. Bartlein, and S. P. Harrison. 2010. Fire history and the Global Charcoal Database: A new tool for hypothesis testing and data exploration. Palaeogeography Palaeoclimatology Palaeoecology 291:52-59.

Reimer, P. J., Bard, E., Bayliss, A., Beck, J.W., Blackwell, P.G., Bronk Ramsey, C., Buck, C.E., Edwards, R.L., Friedrich, M., Grootes, P.M., Guilderson, T.P., Haflidason, H., Hajdas, I., Hatté, C., Heaton, T.J., Hoffmann, D.L., Hogg, A.G., Hughen, K.A., Kaiser, K.F., Kromer, B., Manning, S.W., Niu, M., Reimer, R.W., Richards, D.A., Scott, M.E., Southon, J.R., Turney, C.S.M., van der Plicht, J. 2013. IntCal13 and Marine13 radiocarbon age calibration curves 0-50,000 yr cal BP. Radiocarbon 55:1869-1887.

Schnurrenberger, D., J. Russell, and K. Kelts. 2003. Classification of lacustrine sediments based on sedimentary components. Journal of Paleolimnology 29:141-154.

Shuman, B., W. Thompson, P. Bartlein, and J. W. Williams. 2002. The anatomy of a climatic oscillation: vegetation change in eastern North America during the Younger Dryas chronozone. Quaternary Science Reviews 21:1777-1791.

Teed, R. 2000. A > 130,000-year-long pollen record from Pittsburg Basin, Illinois. Quaternary Research 54:264-274.

Thevenon, F., T. Adatte, J. E. Spangenberg, and F. S. Anselmetti. 2012. Elemental (C/N ratios) and isotopic (d15Norg, d13Corg) compositions of sedimentary organic matter from a high-altitude mountain lake (Meidsee, 2661 m a.s.l. Switzerland): Implications for Lateglacial and Holocene Alpine landscape evolution. Holocene:1-8.

Trowbridge, A. C. 1917. The History of Devils Lake, Wisconsin. Journal of Geology 25:344-372.

Umbanhowar, C. E. 2004. Interaction of fire, climate and vegetation change at a large landscape scale in the Big Woods of Minnesota, USA. Holocene 14:661-676.

Umbanhowar, C. E., P. Camill, and J. A. Dorale. 2011. Regional heterogeneity and the effects of land use and climate on 20 lakes in the big woods region of Minnesota. Journal of Paleolimnology 45:151-166.

Walker, L. R., D. A. Wardle, R. D. Bardgett, and B. D. Clarkson. 2010. The use of chronosequences in studies of ecological succession and soil development. Journal of Ecology 98:725-736.

Wardle, D. A., M. Jonsson, S. Bansal, R. D. Bardgett, M. J. Gundale, and D. B. Metcalfe. 2012. Linking vegetation change, carbon sequestration and biodiversity: insights from island ecosystems in a long-term natural experiment. Journal of Ecology 100:16-30.

Wardle, D. A., L. R. Walker, and R. D. Bardgett. 2004. Ecosystem properties and forest decline in contrasting long-term chronosequences. Science 305:509-513.

Williams, J. J., W. D. Gosling, A. L. Coe, S. J. Brooks, and P. Gulliver. 2011. Four thousand years of environmental change and human activity in the Cochabamba Basin, Bolivia. Quaternary Research 76:58-68.

Wright, H. E. J. 1967. A square-rod piston sampler for lake sediments. Journal of Sedimentary Petrology 37:975-976.

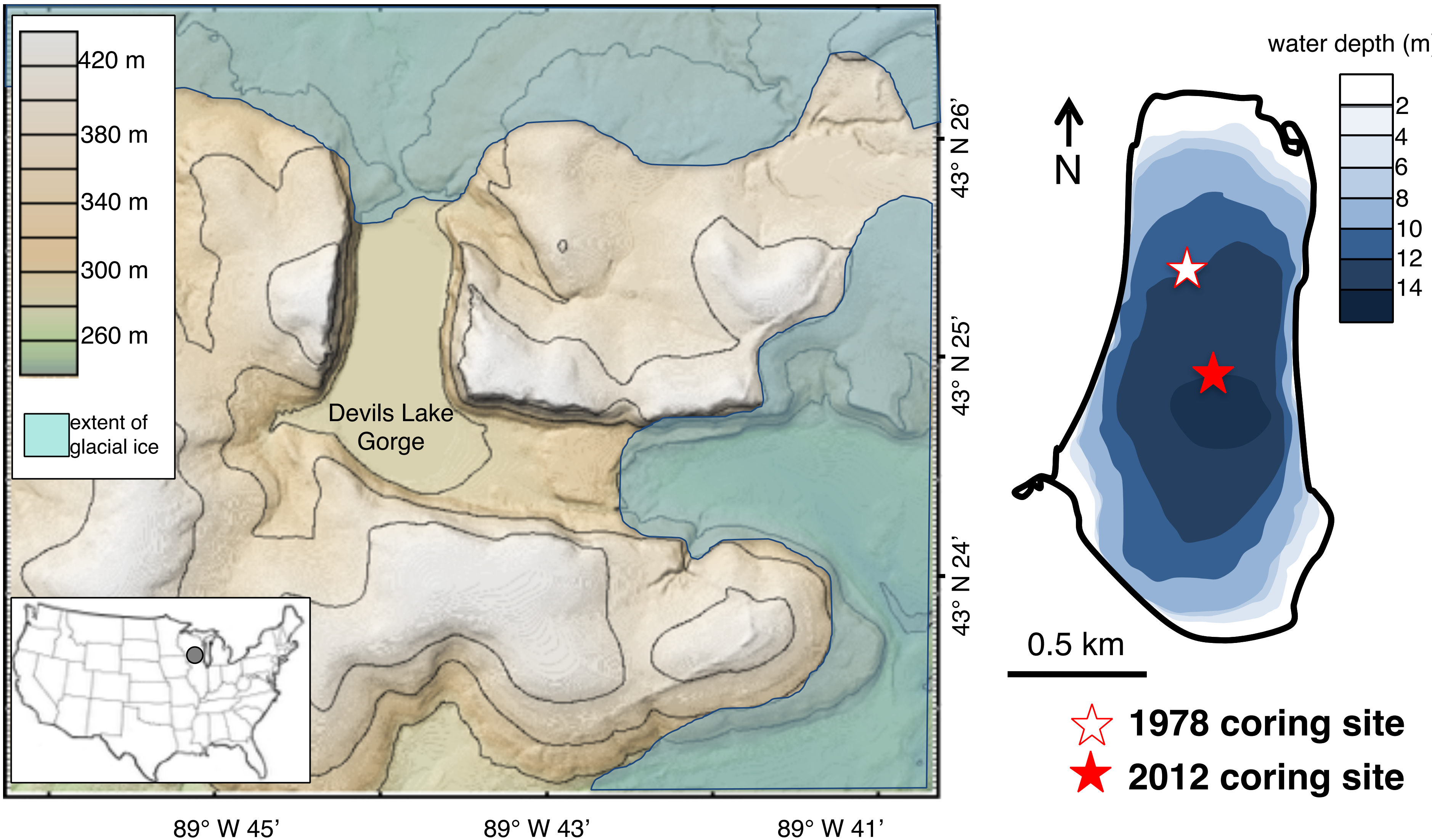
420 m
380 m
340 m
300 m
260 m
extent of glacial ice
Devils Lake Gorge
43° N 26'
43° N 25'
43° N 24'
89° W 45'
89° W 43'
89° W 41'
water depth (m)
2
4
6
8
10
12
14
N
0.5 km
1978 coring site
2012 coring site

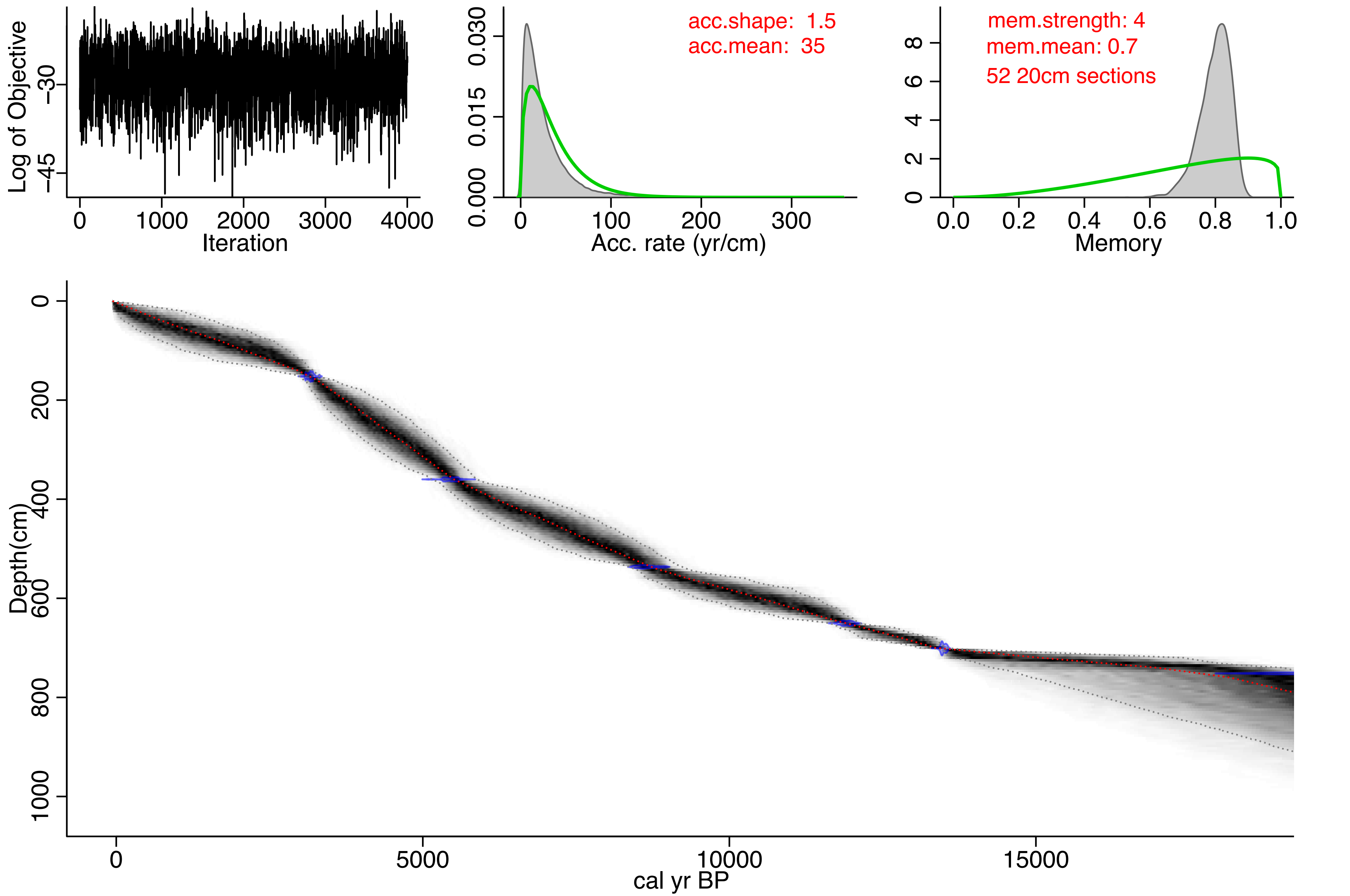

Log of Objective
Iteration
acc.shape: 1.5
acc.mean: 35
Acc. rate (yr/cm)
mem.strength: 4
mem.mean: 0.7
52 20cm sections
Memory
Depth(cm)
cal yr BP

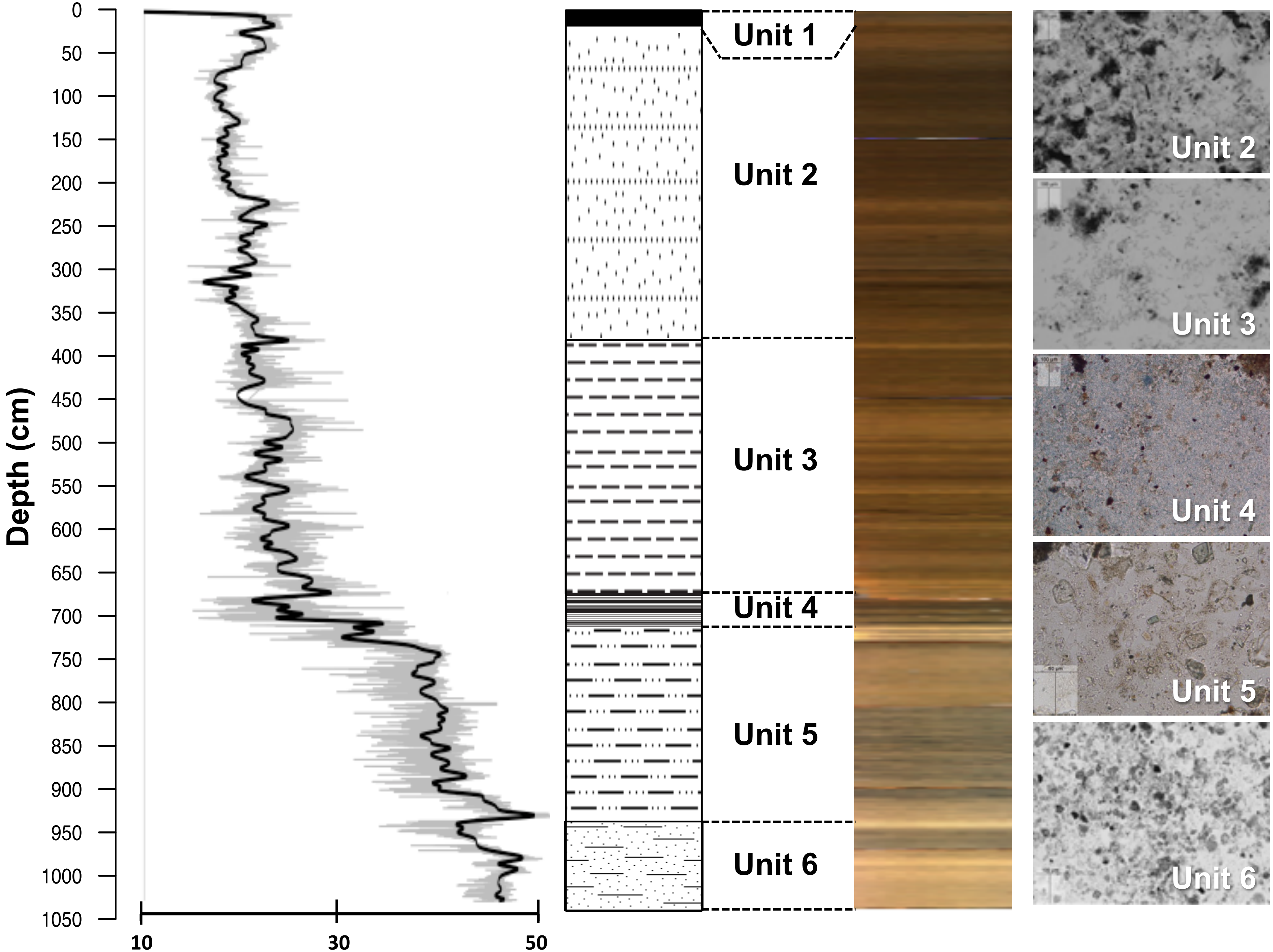

Depth (cm)
0
50
100
150
200
250
300
350
400
450
500
550
600
650
700
750
800
850
900
950
1000
1050
10
30
50
Unit 1
Unit 2
Unit 3
Unit 4
Unit 5
Unit 6

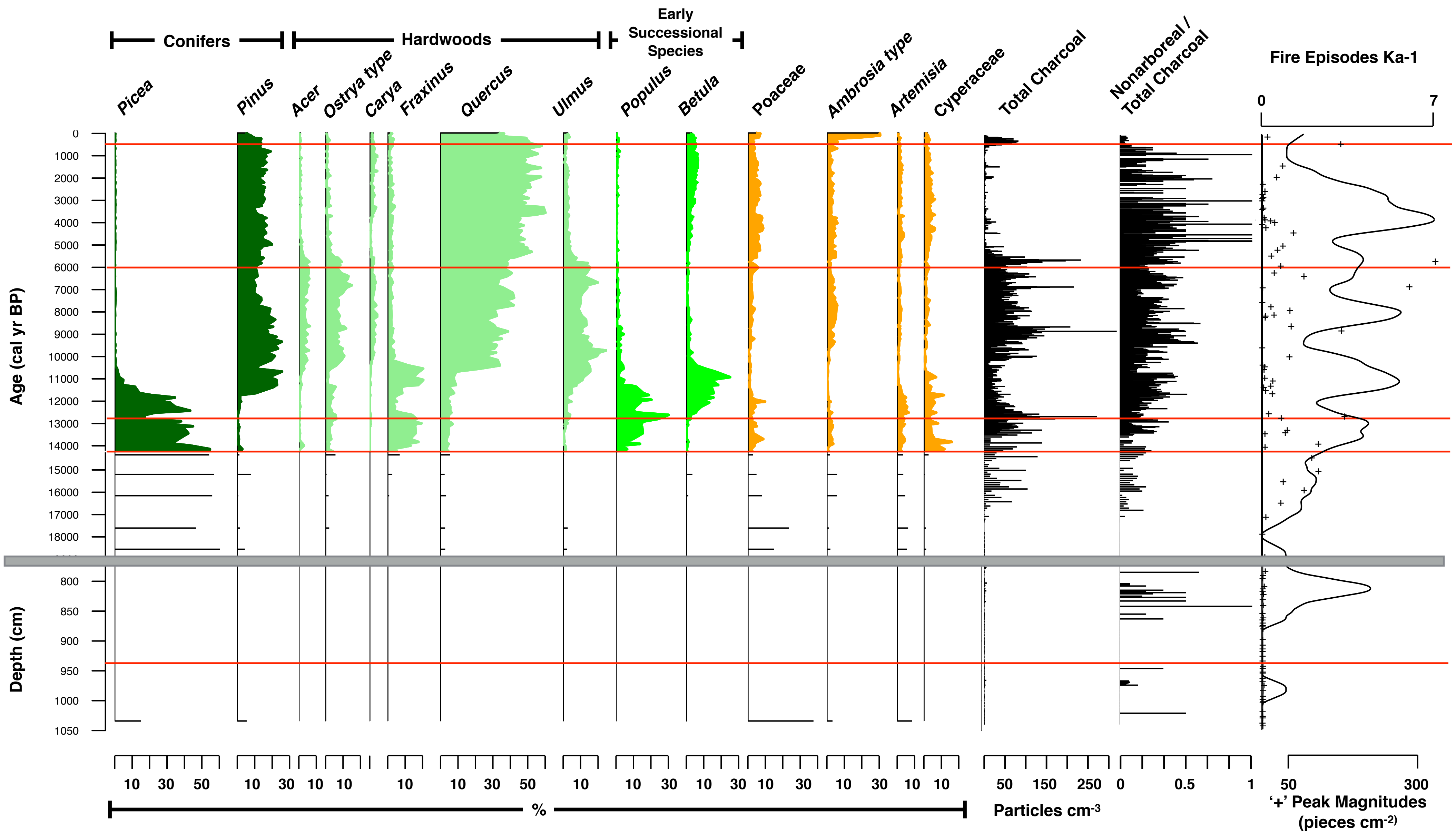

Conifers
Hardwoods
Early Successional Species
Picea
Pinus
Acer
Ostrya type
Carya
Fraxinus
Quercus
Ulmus
Populus
Betula
Poaceae
Ambrosia type
Artemisia
Cyperaceae
Total Charcoal
Nonarboreal / Total Charcoal
Fire Episodes Ka-1
Age (cal yr BP)
Depth (cm)
%
Particles cm-3
'+' Peak Magnitudes (pieces cm-2)

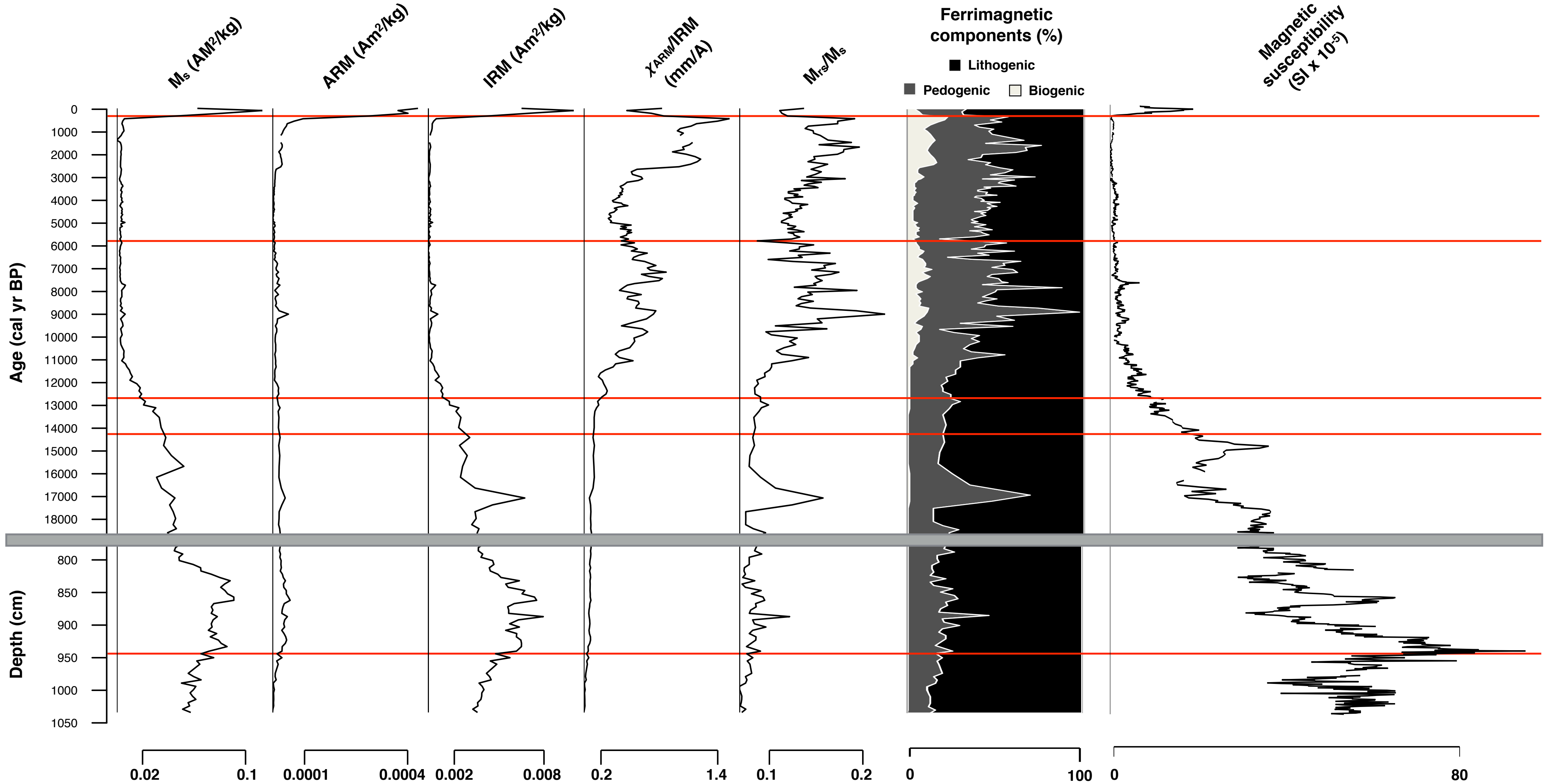

Ms (AM²/kg)
ARM (Am²/kg)
IRM (Am²/kg)
χARM/IRM (mm/A)
Mrs/Ms
Ferrimagnetic components (%)
Lithogenic
Pedogenic
Biogenic
Magnetic susceptibility (SI x 10⁻⁵)
Age (cal yr BP)
Depth (cm)
0.02
0.1
0.0001
0.0004
0.002
0.008
0.2
1.4
0.1
0.2
0
100
0
80

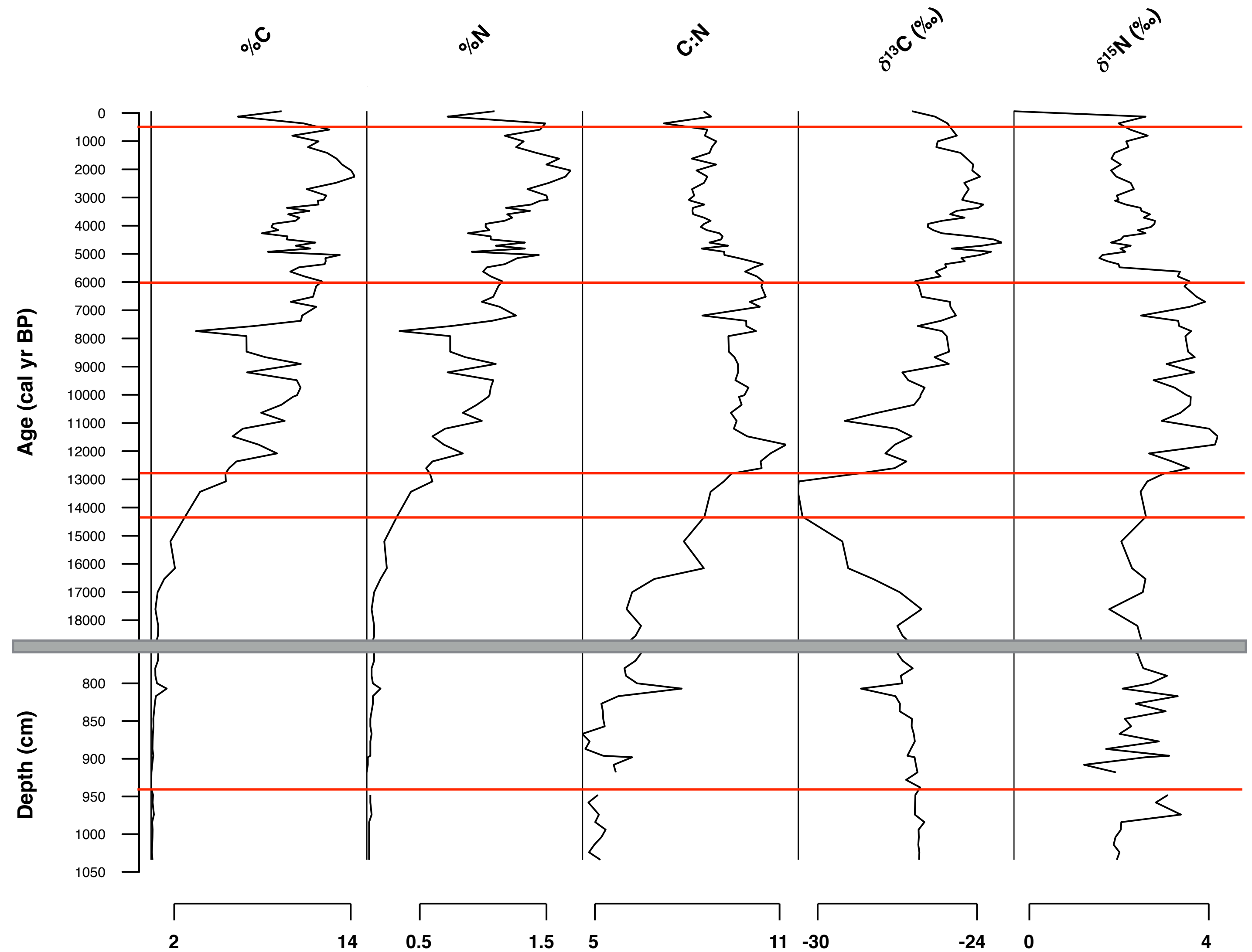

%C
%N
C:N
δ13C (‰)
δ15N (‰)
Age (cal yr BP)
Depth (cm)
0
1000
2000
3000
4000
5000
6000
7000
8000
9000
10000
11000
12000
13000
14000
15000
16000
17000
18000
800
850
900
950
1000
1050
2
14
0.5
1.5
5
11
-30
-24
0
4